27th International Congress on Sound and Vibration
The annual congress of the International Institute of Acoustics and Vibration (IIAV)
11-16 July, 2021
ICSV27

Annual Congress of the International Institute of Acoustics and Vibration (IIAV)

ACOUSTIC BEHAVIOUR OF 3D-PRINTABLE CEMENT MORTARS FUNCTIONALIZED WITH RECYCLED TIRE RUBBER AGGREGATES

Matteo Sambucci and Marco Valente
Department of Chemical and Material Engineering, Sapienza University of Rome, Rome, Italy
INSTM Reference Laboratory for Engineering of Surface Treatments, Department of Chemical and Material Engineering, Sapienza University of Rome, Rome, Italy
email: matteo.sambucci@uniroma1.it

The incorporation of ground tire rubber into cementitious compounds has become a common eco-sustainable practice to confer the materials improved physical-mechanical properties in terms of lightweight, durability, energy absorption, toughness, and thermo-acoustic insulation. Considering the current attention on more comfortable and low-energy structures, the acoustic performances of building materials play a decisive role in improving the quality of life in urban and household environments. This research work aims to reuse end-of-life tires as a granular product in 3D-printable cement mortars, taking advantage of its lightweight and viscoelastic properties to improve the sound attenuation behaviour of the material. Specifically, two grades of granulometry (0-1 mm rubber powder and 2-3 mm rubber granules) were used to replace 100% of the natural aggregates by volume and obtain three printable rubber-cement mixes. Comprehensive acoustic characterization, including sound insertion loss analysis, acoustic flow resistivity, and sound absorption coefficient measurements by impedance tube, was performed to evaluate the influence of rubber particle size on the sound attenuation performance of rubberized mortars. The addition of lightweight and elastomeric rubber particles increases the damping of the material. Indeed, all the rubber-modified mixtures shown comparable/superior insulation properties compared to the reference mixture (0 % rubber), which are modulated by the percentage of fine and coarse polymer fractions incorporated in the matrix. Besides, the rubberized mortars possess excellent sound absorption performances, which are governed by the influence of rubber particles on the microstructural features (porosity and tortuosity) of the cementitious media. The applicability of these mixtures in 3D printing methodologies implies the possibility of developing building-architectural elements with optimized designs for insulating purposes.

Keywords: tire crumb rubber, 3D-printable cement materials, impedance tube, sound insertion loss, sound absorption.

1. Introduction

As documented in the *Environmental noise in Europe-2020* report, drawn up by European Environment Agency (EEA), over 20% of the European population is subject to noise levels which, for long-term exposures, can have deleterious consequences for health and the quality of life [1]. Road traffic, aircraft, railway, industrial activities, and HVAC devices represent the major sources that contribute to environmental noise. Many governments are realizing several strategies to incentivize environmental

noise efficiency and mitigate the potential adverse effects of hazardous acoustic emissions. For instance, in Italy, *Ecobonus2020* legislation [2] proposes tax concessions for the implementation of thermo-acoustic improvement intervention aimed at enhancing the comfort and energy efficiency of buildings. Therefore, noise control has become an engineering sector of strong interest in modern society to develop technological solutions having suitable sound attenuation peculiarities. In the civil-architectural context, a common way to monitor the noise levels is to adopt sound-absorbing or sound-insulating cementitious media, which combine good structural strength properties with high acoustic performance [3]. In the direction of an eco-sustainable approach, some researchers were devoted to study "green" cement-based materials, obtained by functionalization with alternative waste materials or industrial by-products [4].

In the last twenty years, there has been a remarkable interest in using tire crumb rubber (TCR) to replace the natural aggregates in concrete mixes. This practice, commonly referred to as *rubber-concrete* (RC) technology, takes advantage of the viscoelastic nature of polymer inclusions to optimize certain physical-mechanical properties of cementitious matrices, including lightweight, resistance to water absorption and carbonation, mechanical ductility, thermal insulation, vibro-acoustic damping. However, the poor interface adhesion between rubber particles and cement paste is the key factor that affects the reduction in mechanical strength properties. In terms of environmental impact, utilization of waste rubber as cementitious materials constituents represents a clean disposal strategy for end-of-life tires (ELTs) and prevents the excessive consumption of natural raw materials, leading to economic efficiency and sustainable development of the construction industry [5,6]. Although few studies focused on the acoustic properties of RC mixes, attractive sound attenuation behaviour has been demonstrated. *Herrero et al.* [7] observed high airborne noise-damping performances of plaster mortars doped with various volumetric TRC fractions in different particle size gradations. *Zhang and Poon* [8] investigated the improved sound insulation performances of rubberized lightweight concrete by pre-treatment of rubber aggregates with a cementitious coating (65 % increase in noise reduction effect). *Sukontasukkul* [9] demonstrated interesting acoustic absorption properties at high frequencies (> 1000 Hz) of TCR-based precast panels, usable as wall partitions. Based on the detailed literature survey, the engineering qualities of rubber-cement materials suggest a wide-range of possible architectural and civil applications, where high strength is not required. Anti-noise paving blocks, hollow bricks, insulating and anti-shock road barriers, and false façades are some example of possible products, which enhance the lightweight and thermo-acoustic peculiarities of rubberized concrete or mortars.

The authors propose a novel upgrade of RC technology, concerning the development and optimization of TCR-functionalized cementitious compounds suitable for 3D printing processes. In the field of construction engineering, additive manufacturing (AM) has gained considerable interest due to its potential to significantly reduce resource exploitation, labour costs, wastes, and greenhouse gas emissions. Besides, compared to traditional casting concrete methods, the main advantage is that no formworks or moulds are needed and complex building elements and structures can be easily manufactured. In extrusion-based layering method, a fresh cementitious mixture is selectively deposited layer-by-layer by a print head in accordance with commands provided by CAD software to the 3D printer based on crane system or robotic arm [10]. Preliminary research conducted by the authors [11-13] revealed that modification of printable cement mortars with TCR, in addition, to conferring lightweight, mechanical deformability, toughness and heat insulation properties, has positive effects on the print quality of the final product.

To complete the investigation of TCR-cement mortars suitable for AM, an experimental study on the fundamental acoustic properties is presented in this manuscript. Specifically, the sound attenuation performances of printable rubberized compounds, in terms of sound insulation, acoustic absorption, and flow resistivity, were analysed in relation to the size of rubber particles used as alternative aggregate and their replacement ratio in the investigated cementitious formulations.

2. Materials and methods

2.1 Material properties and mix proportions

Two groups of TCR (supplied by *European Tyre Recycling Association*, Belgium) were selected in this study: rubber powder (RP) and rubber granules (RG) were used as fine and coarse fraction, respectively. Size analysis of polymer aggregates was performed by horizontal sieving method in accordance with DIN 66165 standard. The grain size distribution of RP ranges from 125 µm and 710 µm, while RG range from 1 mm and 3 mm. The average density of TCR, measured by *Micromeritics AccuPyc 1330* He-pycnometer, was set to 1.2 g/cm^3.

Four different mix designs were investigated in this research. Control 3D-printable formulation (named here CTR), containing no rubber, consisted of Type I Portland cement (800 kg/m^3), 0-0.4 mm limestone sand (1100 kg/m^3), water (300 kg/m^3), and chemical admixture blend (152 kg/m^3), including Polycarboxylate ether-based superplasticizer and Silica fume-based thixotropic additive. Three TCR-cement mixes were obtained by total volume replacement of sand with rubber aggregates, varying the proportioning level of RP and RG. The amount of cement and admixtures were held constant, to reduce the number of variables and select the optimal rheology and printability of the formulations by changing the water dosage. Ratios of mixture proportioning by volume for rubberized samples are reported below:

- ***RP100* mix:** 100% (v/v) of RP – 0% (v/v) of RG – water-to-cement ratio of 0.325
- ***RP50-RG50* mix:** 50% (v/v) of RP – 50% (v/v) of RG – water-to-cement ratio of 0.312
- ***RP25-RG75* mix:** 25% (v/v) of RP – 75% (v/v) of RG – water-to-cement ratio of 0.287

2.2 3D printing process and specimens manufacturing

Printing test was conducted to investigate the printability of designated mixtures and fabricate the specimens for physical-acoustic characterization. The 3D printing machine is based on a *Comau Robotics* 3-axis robotic arm equipped with a PVC circular nozzle (Ø = 10 mm). The fresh mixes were placed in a vibrating vessel and continuously extruded from the nozzle under air pump pressure of 4 bar and deposition speed of 33 mm/s. For each formulation, pair of six-layers slabs (230 mm x 160 mm x 55 mm) were printed. Extrudability, buildability, and inter-layer adhesion were considered quality indicators to analyse the correct printability of the rubberized mortars. Detailed information about the print quality evaluation can be found in [12,13]. Finally, printed samples were cured for more than 28 days at ambient temperature. After curing, three types of test samples were obtained by cutter machine with circular diamond blade: 48 mm x 48 mm x 22 mm for bulk density evaluation, 40 mm x 40 mm x 10 mm for porosity measurements, and 80 mm x 80 mm x 40 mm for acoustic testing. 3D printing process and the samples manufacturing are illustrated in Fig. 1.

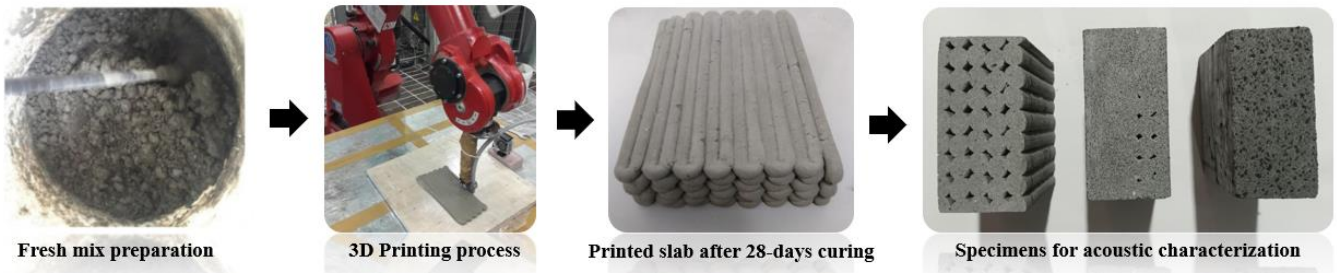

Figure 1: Stages of specimens manufacturing by extrusion-based 3D printing

2.3 Test methods

2.3.1 Physical properties and microstructural analysis

Density and porosity rate are fundamental indicators for the sound attenuation efficiency of cementitious media. Open void ratio affects the acoustic absorption performance of the material. It results from the dissipation of the sound energy into thermal one, due to multiple reflections of acoustic waves within the porous microstructure. On the other hand, acoustic insulation, defined as the ability to reduce the sound transmission through the cement-based medium, can be more suitably achieved when the receiving materials have a high-unit weight or low-Young's modulus as in the case of elastomeric particles used in this study.

According to *BS 1881-114* standard method, bulk density (ρ_b) was computed as the ratio of the oven-dried mass of the specimens (110°C for 48 h) to its geometric volume. For each formulation, the test was performed on four samples and an average value was provided.

Porosity was evaluated in accordance with the vacuum saturation test method (*ASTM C1202* standard). Four specimens for each type of investigated mortar were tested to calculate the mean value. Permeable porosity rate ($A_{\%}$) was obtained as follow: 1) measuring the oven-dried (110°C for 24 h) weight of sample in air (W_{dry}); 2) measuring the mass of the sample after vacuum saturation treatment (W_{sat}) at 0.3 bar for 30 min. into a desiccator; 3) measuring the saturated mass of sample in water (W_{wat}) after total soaking for 3 h. Equation (1) was used to calculate $A_{\%}$:

$$A_{\%} = \left(\frac{W_{sat} - W_{dry}}{W_{sat} - W_{wat}}\right) \times 100 \quad (1)$$

Scanning electron microscopy (SEM) analysis was employed to observe the sample's microstructure and the interfacial transition zone (ITZ) between the rubber aggregates and cement matrix. Small fragments of material were observed with a *Tescan Mira3* FEG-SEM.

2.3.2 Acoustic characterization

A custom-made impedance tube, shown in Fig. (2), was employed to evaluate the acoustic behaviour of cementitious samples, investigating the influence of TCR gradation on the insulating and sound absorption properties of the formulations under study.

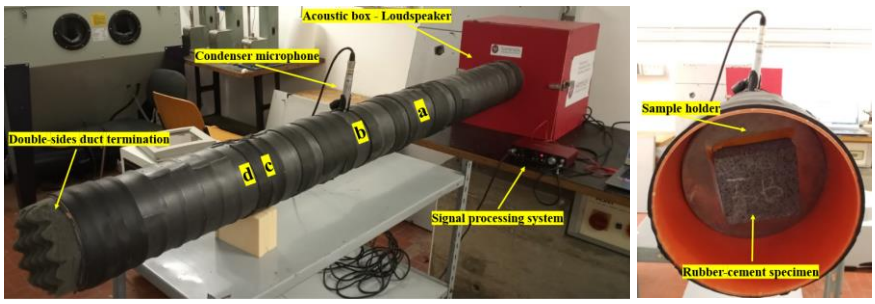

Figure 2: Impedance tube setup (acoustic absorption analysis) and specimen configuration

ISO 10534-2 standard was considered to design and realize the apparatus. Measurements system is constituted by the following parts: 1) two complementary PVC tubes (100 cm length and 16 cm internal diameter) covered with a *Fortlan-Dibi* insulating PET sheath; 2) a trapezoidal wooden acoustic box filled with a *Paulstra-Hutchinson* sound-absorbing PU foam; 3) metallic sample holder; 4) double-sides duct termination (anechoic and absorbent) depending on the type of experimental test; 5) a *YC-7XXUD* thermometer to record the laboratory temperature during the experimentation. Along the tube, four microphone stations, labelled as *a*, *b*, *c*, and *d*, were made at fixed distances from the sample surface (115 cm,

75 cm, 40 cm, and 35 cm, respectively) to modify the experimental configuration based of the acoustic test to be performed. The electro-acoustic line for the supply, acquisition, and processing of the signal consisted of a 30-W *Behringer MPA30BT* loudspeaker, ¼" condenser microphones (*Behringer ECM800*), and a *Focusrite Scarlett 2i4* signal generator. Data acquisition and analysis were performed using *Room EQ Wizard (REW)* software. Acoustic characterization was conducted on two specimens for each formulation. The experimental tests are described in detail below.

Sound insulation performances were determined by Sound Insertion Loss (SIL) measurements in accordance with the recommendations given in *ISO 7235* standard. In SIL experimental setup, the specimen was held in the middle part of the tube between the two microphones located in *a* and *b* stations. At one end of the tube, the loudspeaker, stored in the acoustic box, generated *LOG swept sine* acoustic wave in the frequency range of 50-4000 Hz. The absorbent termination was applied to seal the opposite end of the duct. SIL, in dB, was calculated from sound pressure measurements according to Eq. (2):

$$SIL = Lp_{II} - Lp_{I} \tag{2}$$

where Lp_I is the average sound pressure level gradient in the frequency band when the specimen is installed, and Lp_{II} is the average sound pressure level gradient in the frequency band when the sample is not present.

Standing wave ratio method (*ISO 10534-1* standard) was used to evaluate the sound absorption characteristics of the samples, in terms of α-values. The test material was mounted in the tube end, closed with the reflective side of the termination. The sound source speaker generated a sine wave signal, and a single microphone probe measured the pressure levels in the duct, by varying its distance from the top surface of the specimen. As indicated in *ISO 10534-2* standard, to guarantee propagation of only plane wave across the tube, the usable frequency range depends on the duct internal diameter and the microphone stations used for the acoustic level detection. This experimental facility provides a cut-off frequency of 1260 Hz. For measurements in the range from 100 to 250 Hz, *b* and *d* microphone stations (spaced by 40 cm) were used, while the higher frequency bands (500-1250 Hz) were covered by using *c* and *d* positions (spaced by 5 cm). After generating the required frequency band, the microphone was moved between the two locations (starting from the one closest to the specimen) to measure the minimum and maximum sound pressure amplitude by *Real Time Analyzer (RTA)* tool of *REW*. Normal incident α-coefficient, at the test frequencies 100, 125, 250, 500, 1000, and 1250 Hz, was computed in accordance with Eq. (3):

$$\alpha = \frac{4\times10^{\Delta L/20}}{\left(10^{\Delta L/20}+1\right)^2} \tag{3}$$

where ΔL is the difference between the maximum and minimum sound pressure level values at the analysed frequency.

Acoustical flow resistivity (σ_a) highly affects the sound absorption and sound propagation properties of a pervious medium. Low values indicate scarce sound dissipation, resulting from little friction phenomena inside the material. On the other hand, high σ_a indicates that the material's pores are too closed to permit the air perturbations to flow, therefore low α-values may be expected [14]. In this research, σ_a was determined following the method developed by *Ingard and Dear* [15]. Experimental procedure involves the measurement of sound pressure loss across the specimens, by installing two microphones probes between the sample in *a* and *d* stations. Low-frequency *LOG swept sine* acoustic signal (< 100 Hz) was emitted by the loudspeaker and the sound pressure level in front of the specimen (Lp_i) and near the reflective termination behind the specimen (Lp_t) were recorded by the microphones in *a* and *d* positions, respectively. σ_a, in rayl/m, is defined by Eq. (4):

$$\sigma_a = \frac{\rho_o \times c}{t} \times 10^{(Lp_i - Lp_t)/20} \quad (4)$$

where ρ_0 (1.18 kg/m^3) and c (347.12 m/s) are the density of air and the speed of sound at laboratory temperature of 27°C respectively, and t is the material thickness in m.

3. Results and discussion

3.1 Physical properties and microstructural analysis

Table 1 illustrates the average unit weight and total porosity experimental results. The decrease in ρ_b and $A_{\%}$-values of rubberized mortars can be explained by several competitive factors [11-13]: a) the total replacement of sand with lightweight particles; b) the inclusion of non-porous polymer aggregates in the cement matrix; c) the lower water dosage used for the manufacturing of TCR-cement compounds compared to CTR mix, which minimizes the contribution of capillary porosity in the material; d) the high tendency of non-polar rubber particles to adsorb air on their surface, causing porous TCR-cement interface.

Table 1: Test results for ρ_b and $A_{\%}$

Property	***CTR***	***RP100***	***RP50-RG50***	***RP25-RG75***
ρ_b (kg/m^3)	1927 ± 14	1340 ± 19	1624 ± 10	1468 ± 19
$A_{\%}$ (%)	18.9 ± 0.6	15.9 ± 1.1	21.7 ± 1.3	19.3 ± 0.3

The effect of TCR on density is more pronounced in RP100 mix (- 30%), where the replacement with smaller polymer fraction results in higher rubber content per unit volume. The size gradation also affects the microstructural characteristics of the material. As shown in SEM micrographs reported in Fig. 3, comparing the surface texture of the rubber aggregate, it is possible to notice that the shape of RP is more irregular and jagged than that of RG, caused by the grinding process repeated several times to obtain the desired fineness degree. The high specific surface area of RP promotes better anchoring with the cement paste and improves the material homogeneity [16]. The reverse effect can be observed in the case of RG, where the regular morphology of the coarse particles reduces the interfacial adhesion with the cement, resulting in voids at ITZ. This explains the higher $A_{\%}$ in the "hybrid" rubberized formulations compared to RP100 mix.

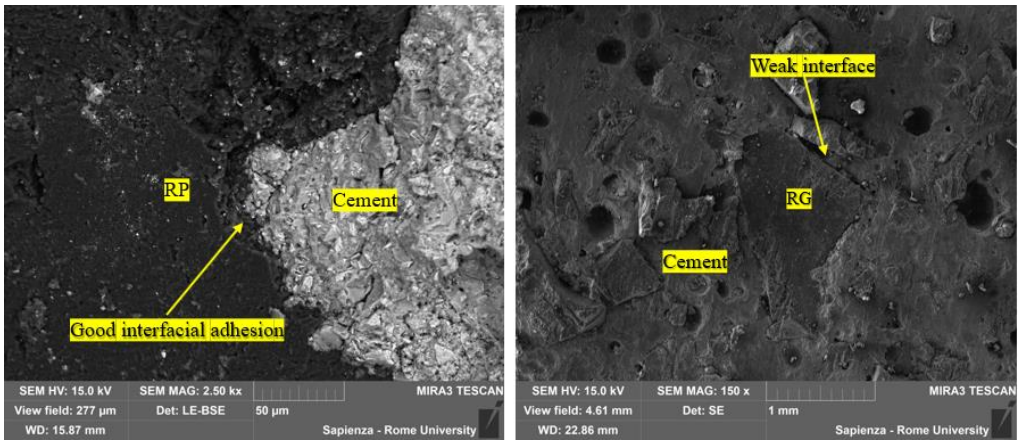

Figure 3: SEM investigation on TCR-cement interface properties

3.2 Acoustic characterization

The trend of SIL for four test cementitious samples is illustrated in Fig. 4. As know, TCR have visco-elasticity properties superior to those of natural aggregates. When subjected to vibration loading, they tend to dissipate the elastic energy, enhancing the damping and soundproof properties of the material [17]. Although comparable insulating behaviour between the denser plain sample and rubberized mortars can be observed, rubber-based modification confers to the cement compound an attractive synergy of lightweight, desirable in terms of thermal insulation and reduction of structural dead loads, and sound retention performances. Depending on the frequency range and rubber particle size, slight differences in acoustic insulation properties can be found. At low-frequency region (< 500 Hz), the most effective result is obtained for RP50-RG50 mix, where a maximum SIL-value of 13 dB (at 250 Hz band) occurs. This phenomenon can be attributed to a proper balance of the coarse and fine polymer fractions in the mix: RP promotes the microstructural homogeneity and RG provide high impediment to sound transmission, due to its great inertia and noticeable capability to dissipate the acoustic energy when vibrating [7,17]. However, the damper effect of larger particles fails in RP25-RG75 sample, which exhibits the worst acoustic performances in the whole frequency spectrum investigated. Probably, a hypothesis of this evidence is based on the deleterious effect of RG-cement interface porosity on sound reflection. At high frequencies, 3D-printable mortars presented higher sound insulation, reaching SIL peak values around 21 dB at 4000 Hz. Over 2000 Hz, better acoustic performances can be achieved in RP100 sample, where the positive influence of fine rubber fraction on the adhesion with the cement matrix minimizes the microstructural defects and promotes the sound attenuation behaviour.

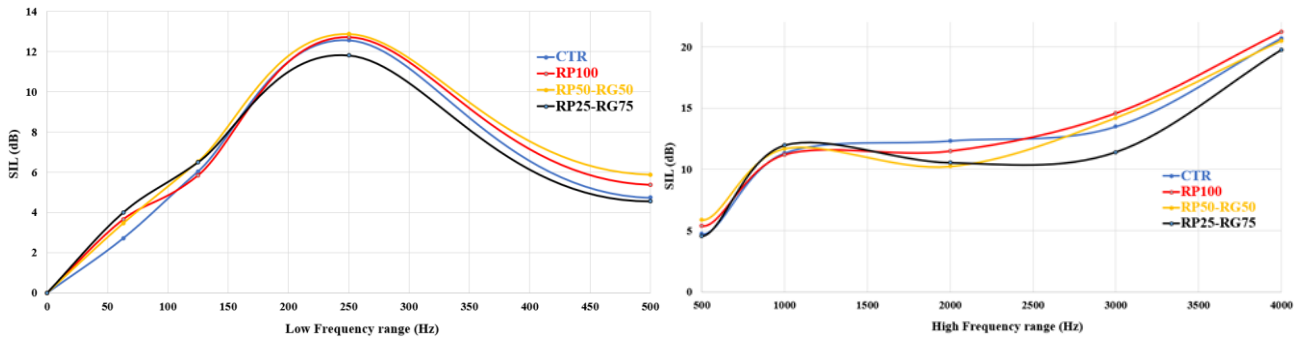

Figure 4: SIL experimental spectra at low-frequency (sx.) and high-frequency (dx.) ranges

Normal incidence α-coefficient spectra and the experimental σ_a-values for different rubberized and plain mortar samples are shown in Fig. 5.

α-values of TCR-cement mixes range from 0.2 and 0.7, which agree to previous works conducted by *Asdrubali et al.* [18] and *Sukontasukkul* [9]. The acoustic absorption capacity is not only related to the energy-dissipative characteristics of rubber but also results from the influence of polymer fillers on the microstructural characteristics of the material, such as open void ratio, inter-connected porosity, and tortuosity [14]. At the low frequency ranges of 100 and 125 Hz, both plain and TCR-based samples exhibited similar α-values, ranging from 0.55 to 0.20. Slight differences can be observed above 250 Hz, where CTR sample provides greater α-coefficient than the TCR-based compounds. By comparing the rubberized samples, marginal divergences in acoustic behaviour can be found, resulting from the effect of particles size on the porosity of the cementitious medium. By increasing the percentage of coarse aggregate (RG) the water requirement to obtain the correct mix rheology is reduced. Low water-to-cement ratios result in less impact of capillary porosity which represents a possible way for the dissipation of acoustic energy into heat, due to the viscous friction of the sound in the internal conduits of the absorber material. This explains the higher α-value in RP100 mix compared to RG-based samples in the 500-1000 Hz

frequency range. Above 1000 Hz, the damping contribution due to the viscoelastic nature of the rubber appears to be the main factor in the higher absorption performance of TCR-cement samples amplifiers than CTR. In this case, the large particle size has a greater impact on the sound attenuation than the fine fraction.

According to *Bies and Hansen* research [3], a common requirement for an efficient acoustic absorber media is that $1 \leq (\sigma_a \cdot t/\rho_0 \cdot c) \leq 4$. By following this condition, the optimal value of σ_a should be in the range $10240 \leq \sigma_a \leq 40960$ for the experimental value of ρ_0, c, and t. As reported in Fig. 5, all the samples investigated widely met this requirement, justifying the potential absorbent effectiveness of the printable mortars. Slight differences in σ_a-values are related to the influence of material's structural micromorphology. As observed by *Gupta et al.* [19], the presence of hydrophobic rubber particles creates additional tortuosity in the cement matrix, hypothetically promoting the visco-thermal mechanism of sound damping. This evidence explains higher σ_a-values of rubberized samples than CTR one. Besides, the knowledge of this acoustic parameter is fundamental to perform finite element method (FEM) simulation and acoustic numerical analysis, in the context of which various poro-acoustic models applied to cementitious media have been proposed [3,14].

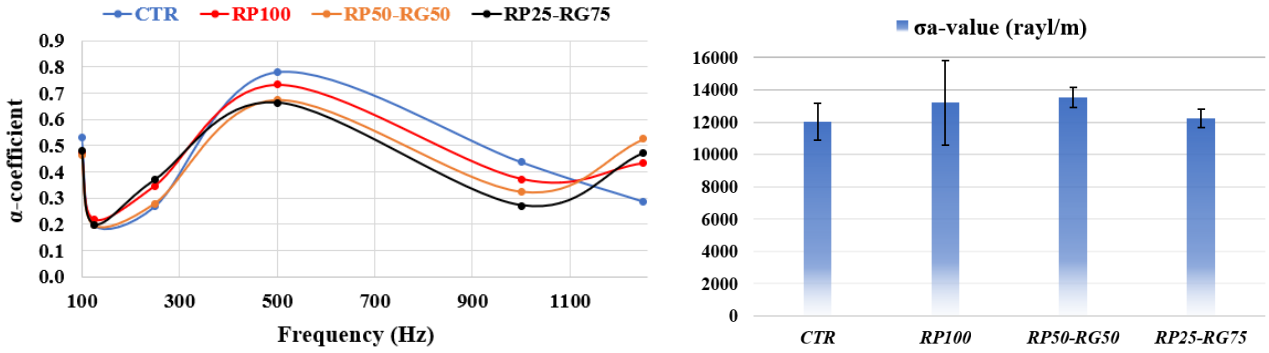

Figure 5: Acoustic absorption experimental spectra (sx.) and σ_a-values (dx.)

.

4. Conclusions

The paper presented the results of the experimental investigation on the acoustic properties of 3D-printable cement mortars functionalized with crumb rubber deriving from end-of-life tires. The incorporation of TCR imparts attractive sound attenuation performances, due to the polyvalent effect of polymer inclusions on insulation and absorption properties. The viscoelastic nature of rubber aggregates enhances the material's damping, resulting in lightweight cementitious compounds with improved sound insulation behaviour. In this regard, particles size gradation is crucial. Optimal balance of the coarse and fine fractions, determined in RP50-RG50 mix, confers to material higher SIL-value at low-middle frequencies (< 500 Hz) than the plain sample, due to the positive synergy between structural compaction and dissipative effect of rubber particles. At high-frequency range, RP100 mix is more effective, probably due to the predominant contribution of material's homogeneity on sound reflection. In terms of acoustic absorption, all the investigated 3D-printable mortars show α-coefficient ranged from 0.20 to 0.78, indicating superior sound attenuation performance compared to traditional concrete materials using in building and architectural fields. This relevant acoustic versatility of rubberized mortars can be exploited to design eco-friendly non-structural elements for noise-abatement purposes, such as noise barriers, insulating bricks, or paving units. In this framework, 3D printing methodology represents an advanced way to develop optimized and functional shapes and geometries, in terms of aesthetics and engineering peculiarities.

REFERENCES

1 European Environmental Agency. *EEA Report No 22/2019.* [Online.] available: https://www.eea.europa.eu/publications/environmental-noise-in-europe.

2 ENEA. *DETRAZIONI FISCALI - Ecobonus, Superbonus e Bonus casa*. [Online.] available: https://www.efficienzaenergetica.enea.it/detrazioni-fiscali.html.

3 Vašina, M., Hughes, D. C., Horoshenkov, K. V. and Lapčík Jr, L. The acoustical properties of consolidated expanded clay granulates, *Applied Acoustics*, **67**(8), 787-796, (2006).

4 Oancea, I., Bujoreanu, C., Budescu, M., Benchea, M. and Grădinaru, C. M. Considerations on sound absorption coefficient of sustainable concrete with different waste replacements, *Journal of Cleaner Production*, **203**, 301-312, (2018).

5 Jie, X. U., Yao, Z., Yang, G. and Han, Q. Research on crumb rubber concrete: From a multi-scale review, *Construction and Building Materials*, **232**, 117282, (2020).

6 Li, Y., Zhang, S., Wang, R. and Dang, F. Potential use of waste tire rubber as aggregate in cement concrete–A comprehensive review, *Construction and Building Materials*, **225**, 1183-1201, (2019).

7 Herrero, S., Mayor, P. and Hernández-Olivares, F. Influence of proportion and particle size gradation of rubber from end-of-life tires on mechanical, thermal and acoustic properties of plaster–rubber mortars, *Materials & Design*, **47**, 633-642, (2013).

8 Zhang, B. and Poon, C. S. Sound insulation properties of rubberized lightweight aggregate concrete, *Journal of cleaner production*, **172**, 3176-3185, (2018).

9 Sukontasukkul, P. Use of crumb rubber to improve thermal and sound properties of pre-cast concrete panel, *Construction and Building Materials*, **23**(2), 1084-1092, (2009).

10 Valente, M., Sibai, A. and Sambucci, M. Extrusion-Based additive manufacturing of concrete products: Revolutionizing and remodeling the construction industry, *Journal of Composites Science*, **3**(3), 88, (2019)

11 Valente, M., Sambucci, M., Sibai, A. and Musacchi, E. Multi-Physics Analysis for Rubber-Cement Applications in Building and Architectural Fields: A Preliminary Analysis, *Sustainability*, **12**(15), 5993, (2020).

12 Sambucci, M., Marini, D., Sibai, A. and Valente, M. Preliminary Mechanical Analysis of Rubber-Cement Composites Suitable for Additive Process Construction, *Journal of Composites Science*, **4**(3), 120, (2020).

13 Sambucci, M., Marini, D. and Valente, M. Tire recycled rubber for more eco-sustainable advanced cementitious aggregate, *Recycling*, 5(2), 11, (2020).

14 Maderuelo-Sanz, R., Barrigón Morillas, J.M., Martín-Castizo, M., Gómez Escobar, V. and Rey Gozalo, G. Acoustical performance of porous absorber made from recycled rubber and polyurethane resin, *Latin American Journal of Solids and Structures*, **10**(3), 585-600, (2013).

15 Nousiainen, E., Hongisto, V. and Lindgren, M. Acoustical characterization of fibrous materials by using measured flow resistivity data, *Proceedings of the 29th International Congress and Exhibition on Noise Control Engineering*, Nice, France, 27-30 August, (2000).

16 Sukontasukkul, P. and Tiamlom, K. Expansion under water and drying shrinkage of rubberized concrete mixed with crumb rubber with different size, *Construction and Building Materials*, **29**, 520-526, (2012).

17 Zhao, J., Wang, X.M., Chang, J.M., Yao, Y. and Cui, Q. Sound insulation property of wood–waste tire rubber composite, *Composites Science and Technology*, **70**(14), 2033-2038, (2010).

18 Asdrubali, F., Baldinelli, G. and D'Alessandro, F. Evaluation of the acoustic properties of materials made from recycled tyre granules, *INTER-NOISE and NOISE-CON Congress and Conference Proceedings*, Istanbul, Turkey, 28-31 August, (2007).

19 Gupta, T., Siddique, S., Sharma, R.K. and Chaudhary, S. Behaviour of waste rubber powder and hybrid rubber concrete in aggressive environment, *Construction and Building Materials*, **217**, 283-291, (2019).